Conformation of L-Tyrosine Studied by Fluorescence-Detected UV-UV and IR-UV Double-Resonance Spectroscopy

*Yoshiya Inokuchi, Yusuke Kobayashi, Takafumi Ito, and Takayuki Ebata**

Department of Chemistry, Faculty of Science, Hiroshima University, Higashi-Hiroshima 739-8526, Japan

Abstract

The laser-induced fluorescence spectrum of jet-cooled L-tyrosine exhibits more than 20 vibronic bands in the 35450–35750 cm^{-1} region. We attribute these bands to eight conformers by using results of UV-UV hole-burning spectroscopy. These isomers are classified into four groups; each group consists of two rotational isomers that have a similar side-chain conformation but different orientations of the phenolic OH. The splitting of band origins of rotational isomers is 31, 21, 5, and 0 cm^{-1} for these groups. IR-UV spectra suggest that conformers belonging to two of the four groups have an intramolecular OH•••N hydrogen bond between the COOH and NH_2 groups. By comparing experimental and theoretical results of L-tyrosine with those of L-phenylalanine, we propose probable conformers of L-tyrosine.

*To whom correspondence should be addressed. E-mail: tebata@hiroshima-u.ac.jp.

1. Introduction

Conformation of amino acids involves the multidimensional structure of proteins. Therefore, many efforts have been made for determining conformation of amino acids in solution.[1, 2] However, poor spectral resolution inherent in condensed phase has frequently caused difficulty in investigation of amino-acid conformation. On the contrary, gas-phase spectroscopy seems to be ideal for the study on the conformation of amino acids. Aromatic amino acids such as tryptophan, phenylalanine, and tyrosine have been the subject of gas-phase investigation, because these molecules are mainly responsible for photochemistry and photophysics of proteins in the near UV region. In the last two decades, a number of important papers on gas-phase spectroscopy of these molecules and their peptides have been reported by many groups.[3–18] These studies have gradually shed light on the "landscape" of conformation for amino acids and peptides.

Here we focus our attention on the study of tyrosine in the gas phase. Levy and co-workers reported a pioneering work of laser-induced fluorescence (LIF) spectroscopy of jet-cooled tyrosine in the 35450–35800 cm^{-1} region.[3] In their LIF spectrum, there appeared 10 vibronic bands, which were divided into two groups around 35525 cm^{-1} and 35650 cm^{-1}. On the basis of the similarity of relative band intensity and band spacing between these groups, they suggested that the appearance of two band groups was caused by the difference in the orientation of the phenolic OH, which provides rotational isomers. (Hereafter we refer to isomers arising from the orientation of the phenolic OH as rotational isomers in this paper.) The splitting of the origin bands for two rotational isomers was ~123 cm^{-1}. More recently, Lindinger et al. demonstrated electronic spectra of tyrosine in He droplets.[19] The tyrosine spectrum in

He droplets shows only four bands. Grace et al. reported resonance two-photon ionization (R2PI) spectroscopy of tyrosine in the 35300–37100 cm^{-1} region.[20] For obtaining tyrosine vapor, they used the laser-desorption technique. They assigned vibronic bands in the R2PI spectrum with the aid of hole-burning experiments and ab initio MO calculation. In the origin band region, the R2PI spectrum is essentially the same as the LIF spectrum measured by Levy's group. However, the interpretation of the spectra was different between the two groups in terms of rotational isomers. Grace et al. ascribed two neighboring bands to rotational isomers with respect to the direction of the phenolic OH. They proposed three couples of rotational isomers for tyrosine, and concluded the splitting of only a few cm^{-1}. Theoretically, Zhang et al. reported ab initio studies of tyrosine.[21] They found 76 conformers, and mentioned that four most stable conformers have an intramolecular O–H•••N hydrogen bond between the COOH and NH_2 groups.

In the present work, we study the structure of jet-cooled L-tyrosine (L-Tyr) by LIF spectroscopy, and fluorescence-detected UV-UV and IR-UV double-resonance spectroscopy. From UV-UV hole-burning spectra, we identify correlation among vibronic bands and obtain the number of conformers of L-Tyr from very congested electronic spectra. IR-UV spectra of L-Tyr enable us to examine conformation of the side chain. From these results, we discuss detailed conformation of the side chain as well as overall structure including the phenolic part.

2. Experimental and computational

In order to produce jet-cooled L-Tyr, a home-made pulsed nozzle plays a key role for suppression of thermal decomposition.[11, 12] We modified the valve design reported by Senkan and Deskin much more simply.[22] We used a solenoid coil of a commercial pulsed nozzle (General Valve, series 9). Instead of the metal valve stem in their design, we used a stem made of poly-imido resin. The length of the stem is 20 mm, and the diameter of the valve orifice is 1 mm. The poppet was also made of poly-imido resin. L-Tyr powder was put into the stem, which was heated to ~90 ˚C by a spiral heater. L-Tyr vapor was injected into a vacuum chamber with He carrier gas; the stagnation pressure was 2 bar. L-Tyr (Tokyo Kasei Kogyo) was used without further purification.

For LIF spectroscopy, an output of a tunable pulsed UV laser (Inrad, Autotracker II (KDP)/ Lambda Physik, Scanmate/ Continuum, Surelite II) was introduced at ~30 mm downstream of the nozzle. Emission induced by the UV laser was collected by a series of lenses and detected by a photomultiplier tube (Hamamatsu Photonics, 1P28). For removing scattered light, we used a long-pass filter between the lenses and the photomultiplier tube. Current from the photomultiplier tube was fed into a boxcar averager (Stanford Research Systems, SR250). Averaged signals were processed by a PC through an analog/digital converter (Stanford Research Systems, SR245) and the GPIB interface. Frequency of the UV laser was calibrated by the opt-galvanic method. This fluorescence detection system was used also for the probe in UV-UV and IR-UV double-resonance spectroscopy. Figure 1 exhibits energy diagrams of double-resonance experiments performed in this study. Frequency of the probe UV laser was fixed to a particular vibronic band in LIF spectra for monitoring

population of a certain state of a conformer. For UV-UV double-resonance spectroscopy, an output of another tunable UV laser (a KDP crystal/ Continuum, ND6000/ Quanta-Ray, GCR250) was introduced to the position ~10 mm upstream of the probe position at ~1 μs prior to the probe laser. Frequency of the UV pump laser was scanned while monitoring fluorescence induced by the probe laser, and depletion of the fluorescence was observed when the pump laser frequency was resonant to a transition of the monitored state. We obtained UV-UV hole-burning spectra as a function of the pump frequency. IR-UV spectra were obtained with a similar experimental scheme. An output of a tunable IR laser was coaxially introduced with the UV probe laser 50 ns prior to the probe pulse. Tunable IR laser light was obtained by difference frequency generation between an output of the dye laser (Continuum, ND6000) and the second harmonics of the Nd:YAG laser (Quanta-Ray, GCR250) with an autotoracker system (Inrad, Autotoracker II ($LiNbO_3$)). Frequency of the probe laser was fixed to a certain transition, and the IR laser frequency was scanned while monitoring the fluorescence signal. We obtained IR depletion spectra in the S_0 state as a function of the IR frequency.

We carried out quantum chemical calculations to obtain probable structures of L-Tyr. Geometry optimization and vibrational analysis of L-Tyr monomer were done at the B3LYP/6-31+G* level of theory. All the calculations were performed by using GAUSSIAN 03.[23] For geometry optimization of L-Tyr, we made initial geometries on the basis of optimized structures of L-phenylalanine (L-Phe) in our previous studies.[11, 12] For comparison of experimental IR spectra with calculated ones, we applied a scaling factor of 0.9744 to vibrational frequencies calculated. This factor was determined so as to reproduce the OH stretching frequency of phenol monomer.

3. Results

A. Electronic spectra

Figure 2 shows LIF spectra of L-Tyr measured in this study. More than 20 vibronic bands appear in the 35450–35750 cm^{-1} region. For convenience, these bands are numbered as seen in Fig. 2. The spectra in Figs. 2a and 2b are measured with different gate positions. The spectrum in Fig. 2a is observed with monitoring a whole time window of fluorescence, whereas the gate position is 12–27 ns from the laser pulse in the spectrum of Fig. 2b. As seen in the figure, spectral features are highly dependent on the gate position monitored; bands **1**, **2**, **3**, **9**, and **10** become very weak with the delayed gate position (Fig. 2b). This result implies that the LIF spectra in Fig. 2 may be ascribed to several species that have different fluorescence lifetimes. Our LIF spectrum in Fig. 2b is very similar to the LIF spectrum measured by Levy and co-workers[3] or the R2PI spectrum reported by Grace et al.[20] Table 1 shows band positions, fluorescence lifetimes, and assignments in the present study. Details of the assignment are mentioned later.

In order to examine correlation among the vibronic bands in Fig. 2a, we observed UV-UV hole-burning spectra with probing bands **1–10**, **14**, and **16–18** in the LIF spectrum. Figures 3b–3d display UV-UV hole-burning spectra obtained by fixing the probe frequencies to bands **4**, **6**, and **18**, respectively. Because the hole-burning spectrum in Fig. 3b shows depletion at positions of bands **4**, **8**, and **19** in the LIF spectrum, these bands belong to a single conformer. Similarly, the hole-burning

spectrum in Fig. 3c shows dips at bands **6**, **12**, and a weak hump appearing on the lower frequency side of band **21**. In Fig. 3d, there are three dips, which are coincident with bands **14**, **18**, and **21** in the LIF spectrum. We also measured the UV-UV hole-burning spectrum with probing band **14**, though it is not shown in Fig. 3. Because this spectrum is almost the same as the spectrum in Fig. 3d, bands **14**, **18**, and **21** are ascribed to the same conformer. Thus, it is concluded that bands **4**, **6**, and **14** are the band origins of the S_1–S_0 transition of different conformers. Hole-burning spectra observed by fixing the probe UV frequencies to other bands show no correlation among vibronic bands in the LIF spectrum. Therefore, vibronic bands other than bands **4**, **8**, **19**, **6**, **12**, **14**, **18**, and **21** are assigned to the band origins of other conformers.

UV-UV hole-burning spectra contain information on vibrational frequencies in the S_1 state and the Franck-Condon overlap between the initial and the final vibronic states. Especially, hole-burning spectra at the low frequency (torsional) region provide spectral features characteristic of conformation of isomers. In Fig. 4, we compare the hole-burning spectra again, where the horizontal axis is the energy relative to the band origin of each isomer. Hole-burning spectra other than those in Fig. 4 show only a single band at the probe positions. As shown in Fig. 4, we can classify the hole-burning spectra into four groups because of spectral similarity. The hole-burning spectra of bands **4** and **6** (Figs. 4a and 4b) show three bands at 39, 52, and 177 cm^{-1} above the origin bands. In the spectra of bands **5** and **7** (Figs. 4c and 4d), a weak band appears at 52 cm^{-1}. For bands **16** and **17** (Figs. 4e and 4f), two noticeable bands are observed at 47 and 69 cm^{-1}. The spectrum of band **14** (Fig. 4g) shows two bands at 44 and 89 cm^{-1}. No other vibronic band in the LIF spectrum shows a hole-burning spectrum similar to that of band **14**. The vibronic bands at ~50 cm^{-1} above the origin

bands were also seen in the R2PI spectrum measured by Grace et al.[20] Ab initio MO calculation demonstrated that there were four low-frequency torsions for L-Tyr: torsion of the entire side chain, torsion of the HOOC(H_2N)CH group about the C_α–C_β bond, COOH torsion, and NH_2 torsion in the order of lower to higher frequency.[20] They assigned the vibronic bands at ~50 cm^{-1} to the torsion of the entire side chain, the lowest-frequency vibration. However, the hole-burning spectra in Figs. 4a and 4b show a band at 39 cm^{-1}, which is lower than 50 cm^{-1}. Therefore, it seems to be difficult to give unambiguous assignments for the low-frequency bands in the present stage.

B. IR spectra

Figure 5 shows IR-UV dip spectra of L-Tyr measured in the 3100–3700 cm^{-1} region. The IR spectra are arranged in the same order as Fig. 4; Figs. 5a–5g display IR spectra observed with probing bands **4**, **6**, **5**, **7**, **16**, **17**, and **14**, respectively. Since L-Tyr is simply *para*-substituted L-Phe by an OH group, IR spectra of L-Tyr will resemble those of phenol and L-Phe.[6, 11, 12, 24] Phenol has the OH stretching band at 3657 cm^{-1}.[24] For L-Phe, the free OH and NH stretching vibrations emerge around 3580 and 3430 cm^{-1}, respectively.[6, 11, 12] L-Phe conformers that have an intramolecular O–H•••N hydrogen bond between the COOH and NH_2 groups show a broad band in the 3200–3300 cm^{-1} region, which is ascribed to the hydrogen-bonded OH stretch. From these studies, one can assign the IR spectra of L-Tyr in Fig. 5 as follows. First, all the spectra in Fig. 5 have a band around 3660 cm^{-1}; this band is the stretching vibration of the phenolic OH. The free OH stretching vibration of the COOH group emerges around 3582 cm^{-1} in the spectra of bands **5**, **7**, **16**, and **17** (Figs. 5c–5f). Weak bands at

3413 and 3431 cm^{-1} in the spectra of bands **4**, **6**, and **14** (Figs. 5a, 5b, and 5g) are the asymmetric NH stretching vibration of the NH_2 group. Finally, relatively broad bands in the region of 3200–3300 cm^{-1} (Figs. 5a, 5b, and 5g) are attributed to the hydrogen-bonded OH stretching vibration of the COOH group.

C. Thermal decomposition of tyrosine

The use of the poly-imido nozzle enables us to suppress thermal decomposition effectively. However, we found that the LIF spectrum drastically changed under a higher temperature condition (> 95 ˚C) even by using the poly-imido nozzle. It is necessary to consider the effect of thermal decomposition of L-Tyr. One of the possible decomposition species of L-Tyr is tyramine, which is produced with the elimination of CO_2.[13] Figure 6 compares our LIF spectrum of L-Tyr (Fig. 6a) with the LIF spectrum of tyramine (Fig. 6b) reported by Levy and co-workers.[25] The LIF spectrum of tyramine has six strong bands in this region; these bands were assigned to the origin bands of different conformers. These band positions are completely coincident with bands **1**, **2**, **3**, **9**, **10**, and **13** in our LIF spectrum. We have measured an IR-UV spectrum by monitoring band **3**. The IR spectrum shows no band assignable to the OH stretching vibration of the COOH group, suggesting that CO_2 is eliminated from L-Tyr. Therefore, we ascribe bands **1**, **2**, **3**, **9**, **10**, and **13** in the LIF spectrum to tyramine produced by thermal decomposition of L-Tyr. In order to confirm our assignment, we have observed an R2PI spectrum with a time-of-flight mass spectrometer under a high nozzle temperature condition (~130 ˚C).[26] The measurement has been done with monitoring the ion at m/Z = 137, corresponding to $(tyramine)^+$. The R2PI spectrum exhibits six bands at positions the same as those of

bands **1**, **2**, **3**, **9**, **10**, and **13**. This observation supports the validity of our assignment of tyramine. Difference between L-Tyr and tyramine is seen also in the fluorescence lifetimes; the lifetimes of tyramine (< 3 ns) are shorter than those of L-Tyr (Table 1).

D. Optimized structures of L-Tyr

It would be quite time-consuming work to search overall potential energy surface of L-Tyr by ab initio MO calculation. In fact, Zhang et al. found 76 conformers of L-Tyr.[21] In this study, we try to examine L-Tyr theoretically with less efforts by considering results of L-Phe. Simon and co-workers reported nine minimum-energy structures of L-Phe derived from geometry optimization.[6] Among them, six conformers (A–E and X) were found under the jet-cooled condition.[6, 11, 12] Thus, we use the structure of these six conformers of L-Phe for ab initio MO calculation of L-Tyr. Considering the orientation of the phenolic OH group, we had 12 initial geometries for geometry optimization of L-Tyr. With these initial geometries, we obtain 12 stable conformers, which are shown in Fig. 7. The side-chain conformations are almost kept in the course of geometry optimization. Therefore, one can distinguish these L-Tyr conformers by the notation "X-*n*"; the first character "X" represents that this conformer has a side-chain conformation similar to that of conformer "X" of L-Phe; the number "*n*" is for identifying the rotational isomer about the phenolic OH group. Table 2 shows total energies relative to that of the most stable conformer (X-1) calculated at the B3LYP/6-31+G* level. Rotational isomers that have a similar side-chain conformation have energies almost the same as each other. For L-Tyr, averaged values of total energies for conformers A–E and X are 603, 33, 423, 328, 438, and 61 cm^{-1}; conformers B and X are the most stable, and the ordering of the stability is B, X,

D, C, E, A. In Table 2, relative energies of L-Phe calculated at the same level (B3LYP/6-31+G*) are also displayed in cm^{-1}.[6] The ordering of stability (B, X, D, C, E, A) is completely the same as that of L-Tyr, and even the energy difference between the conformers are quite similar to the case of L-Tyr. These results suggest that the substitution of an OH group at *para* position of L-Phe does not affect largely the relative stability of conformers. Therefore, it is reasonable to consider L-Tyr conformers derived from experimentally-confirmed six conformers of L-Phe. In Table 3, frequencies of six lowest-frequency vibrational modes are collected for each conformer of L-Tyr. Rotational isomers with a similar side-chain conformation have almost the same vibrational frequencies; the difference is at most only 7 cm^{-1}. Conformers of L-Tyr have low-frequency modes characteristic of the side-chain conformation; these modes are not highly dependent on the orientation of the phenolic OH group.

4. Discussion

As mentioned above, L-Tyr conformers have low-frequency vibrations characteristic of the side-chain conformation in the S_0 state (Table 3). This can be applied to vibrations in the S_1 state if the molecular structure does not change largely by the electronic excitation. Levy and co-workers reported dispersed emission spectra of tyrosine observed by the excitation of the band origins.[3] The dispersed emission spectra show no broad, red-shifted emission, suggesting that intramolecular exciplex formation or large structural change does not occur for tyrosine in the origin region of the S_1 state. Therefore, if side-chain conformations of different conformers are similar to each other in the S_0 state, hole-burning spectra in the low-frequency region of the S_1

state may probably resemble each other. From these considerations, we ascribe the vibronic bands giving similar hole-burning spectra to rotational isomers due to different orientations of the phenolic OH but with a similar side-chain conformation. Here we tentatively label groups of rotational isomers as **k**, **l**, **m**, and **n** (see Table 1). For example, we label isomers providing bands **4** and **6** as $\mathbf{k}_1$ and $\mathbf{k}_2$. The splitting of groups **k**–**n** is 31, 21, 0, and 5 cm^{-1}, respectively. (For group **m**, the splitting may be too small to be separated in our spectrum.) These splittings are comparable to that of 4-propylphenol (12 cm^{-1}).[27]

The IR-UV spectra of groups **k** (Figs. 5a and 5b) and **m** (Fig. 5g) show similar spectral features with a broad band in the 3200–3300 cm^{-1} region and a weak band around 3420 cm^{-1}. However, the band positions are noticeably different between groups **k** and **m**. Group **k** shows the hydrogen-bonded OH stretching band of COOH at ~3285 cm^{-1} and the asymmetric NH stretching band of NH_2 at 3413 cm^{-1}. Group **m** has corresponding bands at 3232 and 3431 cm^{-1}, respectively. A similar disagreement of the band position was observed also for L-Phe.[6, 11, 12] Conformer B of L-Phe has the hydrogen-bonded OH band at 3280 cm^{-1} and the asymmetric NH band at 3411 cm^{-1}; these frequencies are coincident with those of group **k** of L-Tyr. The IR spectrum of conformer X of L-Phe exhibits bands at 3235 and 3428 cm^{-1}, almost the same as the band position of group **m** of L-Tyr. Therefore, conformers of L-Tyr belonging to groups **k** and **m** have the side-chain conformations similar to conformers B and X of L-Phe, respectively. This trend of the band position appears also in calculated IR spectra of L-Tyr. Figure 8 displays comparison of the IR-UV spectra of groups **k** (Figs. 8a and 8b) and **m** (Fig. 8e) with calculated ones of the stable conformers of B-1 and B-2 (Figs. 8c and 8d) and X-1 and X-2 (Figs. 8f and 8g). The calculated spectra well

reproduce the position of the stretching band of the phenolic OH group around 3655 cm^{-1}. On the other hand, the band positions of the hydrogen-bonded OH and the asymmetric NH vibrations are largely different between the observed and calculated spectra. However, the frequencies of the hydrogen-bonded OH band of B-1 and B-2 (3320 and 3319 cm^{-1}) are obviously higher than those of X-1 and X-2 (3293 and 3297 cm^{-1}). The asymmetric NH bands of B-1 and B-2 are located at a frequency (3475 and 3476 cm^{-1}) lower than those of X-1 and X-2 (3491 cm^{-1}). Therefore, conformers of groups **k** (bands **4** and **6**) and **m** (band **14**) are assignable to conformers B-*n* and X-*n* in Fig. 7, respectively. Since conformer B-1 has a total energy and a vibrational structure similar to those of conformer B-2, the respective assignments of group **k** bands (bands **4** and **6**) to B-1 or B-2 is not possible at present. Therefore, we refer to bands **4** and **6** in the LIF spectra as B and B' (see Table 1), which means that these conformers have a side-chain conformation similar to that of conformer B of L-Phe, and that conformers B and B' are the rotational isomers with respect to the direction of the phenolic OH. In the case of group **m**, no splitting is observed in the LIF spectra. Thus, the band of group **m** (band **14**) is assigned to "X, X'" in Table 1.

Moreover, one can reduce possible conformers of groups **l** and **n** of L-Tyr to conformers D-*n* and E-*n* on the basis of total energies and IR spectra. First there are four candidates for groups **l** and **n**: conformers A-*n*, C-*n*, D-*n*, and E-*n*. Among them, conformers A-*n* are excluded from the candidates, because conformers A-*n* are much more unstable than other conformers (Table 2).[28] Since conformers C-*n*, D-*n*, and E-*n* have a total energy similar to each other (Table 2), all the conformers could be the structure of groups **l** and **n** in terms of the total energy. As seen in Fig. 7, only conformers C-*n* have a weak OH•••π hydrogen bond between the COOH group and the

aromatic ring. A sign of the OH•••π hydrogen bond in conformers C-*n* emerges in IR spectra calculated. Figure 9 shows comparison of the IR-UV spectra measured at bands **5**, **7**, **16**, and **17** with IR spectra calculated for D-*n*, E-*n*, and C-*n* in the free OH stretching region (3400–3700 cm^{-1}). The OH stretching vibration of the COOH group of conformers C-*n* is calculated to be 3569 cm^{-1}, lower than those of conformers D-*n* and E-*n* (3582 and 3583 cm^{-1}, respectively). In the IR-UV spectra of L-Tyr, groups **l** (bands **5** and **7**) and **n** (band **16** and **17**) have the OH stretching band of the COOH group around 3582 cm^{-1}, indicating that conformers of groups **l** and **n** do not have any hydrogen bond like the OH•••π bond. Therefore, possible structures of groups **l** and **n** of L-Tyr are conformers D-*n* and E-*n*. This result is supported by the experimental results of L-Phe; conformer C of L-Phe has the carboxyl OH band at 3567 cm^{-1}, which is lower than those of conformer D (3579 cm^{-1}).[6] Finally, it is necessary to assign groups **l** and **n** respectively to conformers D-*n* or E-*n*. In the present stage, there is no unambiguous evidence for the assignment. However, we can propose that group **l** is ascribed to conformers D-*n*, and that group **n** is to E-*n* by the following consideration. One is the relative band intensity for groups **l** and **n** in the LIF spectra. As seen in Fig. 2, bands of group **l** (bands **5** and **7**) are stronger than those of group **n** (bands **16** and **17**); the relative intensity is 1:0.75 between groups **l** and **n**. Assuming Boltzmann distribution at 363 K, which is the temperature of the sample source, and using the total energy calculated for conformers D-*n* and E-*n*, the relative population of conformers D-*n* and E-*n* is estimated at 1:0.65, comparable to the result derived from the band intensity. In the case of L-Phe, the order of the band position in the electronic spectra is B, D, X, and E from lower to higher frequency.[6, 11, 12] If this order is kept for L-Tyr, groups **l** and **n** correspond to conformers D-*n* and E-*n*, respectively.

The validity of the assignment to rotational isomers with respect to the phenolic OH can be found in the relative intensity of the origin bands in our LIF spectra and the electronic spectra reported in the previous studies. Figure 10 reproduces the LIF spectrum measured by Levy and co-workers[3] (Fig. 10b) and the R2PI spectrum by Grace et al.[20] (Fig. 10c) with our LIF spectrum (Fig. 10a). Since our DFT calculations of L-Tyr predict similar stability for two rotational isomers, the population of two rotational isomers would be almost the same as each other. In our LIF spectrum (Fig. 10a), one can find that the band intensities of conformers B and B' are similar to each other. Also for conformers D and D' and conformers E and E', the similarity of the band intensity can be seen in our LIF spectrum. Since no other strong band comparable to band **14** is found in the spectrum, we suggest that the two origin bands of conformers X and X' are overlapped at the position of band **14**. Since the spectrum of Levy's group was measured under a saturated condition by use of a strong UV laser, the weak bands in our spectrum are enhanced in their spectrum. However, the situation that the band intensity for two rotational isomers are almost the same is kept also in their spectrum. In the R2PI spectrum, relative intensities of bands A and B' (corresponding to B and B' in our spectrum) are weak, which may be due to the different generation method or the ionization efficiency. Despite this difference, the band intensity for the two rotational isomers is almost the same.

5. Conclusion

We have applied fluorescence-detected UV-UV and IR-UV double resonance spectroscopy to jet-cooled L-tyrosine. The UV-UV hole-burning spectra have enabled us to discriminate four groups **k**–**n** of rotational isomers caused by the orientation of the phenolic OH. Each group possesses a similar side-chain conformation, which has been verified by the IR-UV spectra. The IR-UV spectra of these conformers show that conformers of groups **k** and **m** have an intramolecular O–H•••N hydrogen bond between the COOH and NH_2 groups. By comparing the experimental and theoretical results of L-tyrosine with those of L-phenylalanine, we have concluded that conformers of L-tyrosine existing under jet-cooled condition have side-chain conformations similar to conformers B, D, E, and X of L-phenylalanine.

Acknowledgment

We gratefully acknowledge encouraging discussion with Prof. Elliot R. Bernstein in Colorado State University. We also thank Profs. C. Jouvet and C. Dedonder-Lardeux in Universite Paris-Sud for measurement of the R2PI spectrum of tyramine. This study is supported by the Grant-in-Aids for Scientific Research (18205003 and 18685001) by the Ministry of Education, Science, Sports, and Culture, Japan. T.E. thanks the support of Satake foundation.

Table 1. Band position, lifetime, assignment for vibronic bands in the LIF spectra, and band labeling in the previous papers.

Band	Position (cm^{-1})	Fluorescence Lifetime (ns)	Assignment[a]	Label 1[b]	Label 2[c]
1	35465	2.8	tyramine		
2	35477	2.1	tyramine		
3	35484	2.1	tyramine		
4 (**k**$_1$)	35491	7.1	B	A	A
5 (**l**$_1$)	35516	5.0	D	B	B
6 (**k**$_2$)	35522	5.7	B’	C	B’
7 (**l**$_2$)	35537	4.5	D’	D	C
8	35543	-	(B)		
9	35548	2.4	tyramine		
10	35560	2.5	tyramine		
11	35567	-	-		
12	35573	3.6	(B’)		
13	35581	2.1	tyramine		
14 (**m**)	35612	7.9	X, X’	E	D’
15	35633	4.9	-	G	G
16 (**n**$_1$)	35640	4.1	E	H	E
17 (**n**$_2$)	35645	3.5	E’	I	E’
18	35656	6.6	(X, X’)	J	
19	35667	-	(B)		
20	35678	-	-		
21	35701	-	(X, X’)		

[a] Assignments in parentheses show that these bands correlate with origin bands of corresponding conformers.
[b] Ref. 3.
[c] Ref. 20.

Table 2. Total energy of stable conformers of L-Tyr and L-Phe calculated at the B3LYP/6-31+G* level of theory.

Conformer	Relative Energy (cm^{-1})		
	L-Tyr[a]		L-Phe[b]
A-1	595	(603)	600
A-2	611		
B-1	37	(33)	0
B-2	28		
C-1	429	(423)	394
C-2	417		
D-1	329	(328)	334
D-2	327		
E-1	435	(438)	406[c]
E-2	441		
X-1	0	(61)	54
X-2	121		

[a]Zero-point energies are included. The numbers in the parentheses show the averaged values for each pair of rotational isomers.

[b]Ref. 6.

[c]Simon and co-workers assigned band E of L-Phe to structure IV in Ref. 6. However, we have reassigned band E to structure VII of Ref. 6 on the basis of IR spectroscopy (Ref. 12). This is the energy calculated for structure VII in Ref. 6.

Table 3. Vibrational frequency of stable conformers of L-Tyr.[a]

Mode No.	Frequencies (cm^{-1})											
	A-1	A-2	B-1	B-2	C-1	C-2	D-1	D-2	E-1	E-2	X-1	X-2
1	25	32	41	42	22	26	39	39	36	35	41	39
2	42	44	48	48	39	38	44	45	46	47	51	51
3	64	64	63	63	51	52	58	58	58	58	76	75
4	82	82	86	86	73	74	85	85	67	67	88	87
5	161	161	169	170	146	147	160	160	165	165	170	170
6	212	211	186	186	236	236	207	207	183	183	209	208

[a] Six lowest-frequency modes are shown for each stable conformer. The scaling factor is not applied to the frequencies in this table.

Figure Captions

Figure 1. Energy diagram and a scheme of double-resonance spectroscopy performed in this study: (a) UV-UV, (b) IR-UV.

Figure 2. LIF spectra of jet-cooled L-tyrosine measured with monitoring whole time window of fluorescence (a) and with monitoring a delayed gate position of 12–27 ns from the laser pulse (b).

Figure 3. (a) Reproduction of the LIF spectrum in Fig. 2a. (b–d) UV-UV hole-burning spectra observed with probing bands **4**, **6**, and **18** in the LIF spectrum.

Figure 4. UV-UV hole-burning spectra observed with probing bands **4**, **6**, **5**, **7**, **16**, **17**, and **14** in the LIF spectrum (a–g). The abscissa axis represents the energy relative to the transition energy of the origin bands.

Figure 5. IR spectra observed with probing bands **4**, **6**, **5**, **7**, **16**, **17**, and **14** in the LIF spectrum (a–g).

Figure 6. Comparison of the LIF spectrum of L-Tyr measured in this study (a) with the LIF spectrum of tyramine by Levy and co-workers (b) (Ref. 25).

Figure 7. Optimized structures of L-Tyr at the B3LYP/6-31+G* level.

Figure 8. IR-UV spectra observed at bands **4**, **6**, and **14** (a, b, and e). IR spectra calculated for conformers B-1, B-2, X-1, and X-2 (c, d, f, and g). For calculated frequencies, a scaling factor of 0.9744 is used.

Figure 9. IR-UV spectra observed at bands **5**, **7**, **16**, and **17** (a, b, e, and f). IR spectra calculated for conformers D-1, D-2, E-1, E-2, C-1, and C-2 (c, d, g–j). For calculated frequencies, a scaling factor of 0.9744 is used. The dotted line is drawn at 3569 cm^{-1}.

Figure 10. Comparison of electronic spectra of tyrosine. (a) LIF spectrum measured in this study. (b) LIF spectrum by Levy and co-workers (Ref. 3). (c) R2PI spectrum by Grace et al. (Ref. 20).

References and notes

[1] Eftink, M. R.; Ghiron, C. A. *Biochemistry* **1976**, *15*, 672.

[2] Ross, J. B. A.; Rousslang, K. W.; Brand, L. *Biochemistry* **1981**, *20*, 4361.

[3] Martinez III, S. J.; Alfano, J. C.; Levy, D. H. *J. Mol. Spectrosc.* **1992**, *156*, 421.

[4] Snoek, L. C.; Kroemer, R. T.; Hockridge, M. R.; Simons, J. P. *Phys. Chem. Chem. Phys.* **2001**, *3*, 1819.

[5] Snoek, L. C.; Kroemer, R. T.; Simons, J. P. *Phys. Chem. Chem. Phys.* **2002**, *4*, 2130.

[6] Snoek, L. C.; Robertson, E. G.; Kroemer, R. T.; Simons, J. P. *Chem. Phys. Lett.* **2000**, *321*, 49.

[7] Oomens, J.; Polfer, N.; Moore, D. T.; van der Meer, L.; Marshall, A. G.; Eyler, J. R.; Meijer, G.; von Helden, G. *Phys. Chem. Chem. Phys.* **2005**, *7*, 1345.

[8] Macleod, N. A.; Butz, P.; Simons, J. P.; Grant, G. H.; Baker C. M.; Tranter, G. E. *Phys. Chem. Chem. Phys.* **2005**, *7*, 1432.

[9] Robertson, E. G.; Simons, J. P. *Phys. Chem. Chem. Phys.* **2001**, *3*, 1.

[10] Lee, K. T.; Sung, J.; Lee, K. J.; Kim, S. K. *J. Chem. Phys.* **2002**, *116*, 8251.

[11] Hashimoto, T.; Takasu, Y.; Yamada, Y.; Ebata, T. *Chem. Phys. Lett.* **2006**, *421*, 227.

[12] Ebata, T.; Hashimoto, T.; Ito, T.; Inokuchi, Y.; Altunsu, F.; Brutschy, B.; Tarakeshwar, P. *Phys. Chem. Chem. Phys.* **2006**, *8*, 4783.

[13] Cohen, R.; Brauer, B.; Nir, E.; Grace, L.; de Vries, M. S. *J. Phys. Chem. A.* **2000**, *104*, 6351.

[14] Unterberg, C.; Gerlach, A.; Schrader, T.; Gerhards, M. *J. Chem. Phys.* **2003**, *118*, 8296.

[15] Philips, L. A.; Webb, S. P.; Martinez III, S. J.; Fleming, G. R.; Levy, D. H. *J. Am. Chem. Soc.* **1988**, *110*, 1352.

[16] Wilson, K. R.; Jimenez-Cruz, M.; Nicolas, C.; Belau, L.; Leone, S. R.; Ahmed, M. *J. Phys. Chem. A* **2006**, *110*, 2106.

[17] Dian, B. C.; Longarte, A.; Mercier, S.; Evans, D. A.; Wales, D. J.; Zwier, T. S. *J. Chem. Phys.* **2002**, *117*, 10688.

[18] Chin, W.; Dognon, J.-P.; Piuzzi, F.; Tardivel, B.; Dimicoli, I.; Mons, M. *J. Am. Chem. Soc.* **2005**, *127*, 707.

[19] Lindinger, A.; Toennies, J. P.; Vilesov, A. F. *J. Chem. Phys.* **1999**, *110*, 1429.

[20] Grace, L. I.; Cohen, R.; Dunn, T. M.; Lubman, D. M.; de Vries, M. S. *J. Mol. Spectrosc.* **2002**, *215*, 204.

[21] Zhang, M.; Huang, Z.; Lin, Z. *J. Chem. Phys.* **2005**, *122*, 134313.

[22] Senkan, S. M.; Deskin, S. C. *Rev. Sci. Instrum.* **1997**, *68*, 4286.

[23] Frisch, M. J. et al. *Gaussian 03 Revision B.05*, Gaussian, Inc., Pittsburgh PA, 2003.

[24] Tanabe, S.; Ebata, T.; Fujii, M.; Mikami, N. *Chem. Phys. Lett.* **1993**, *215*, 347.

[25] Martinez III, S. J.; Alfano, J. C.; Levy, D. H. *J. Mol. Spectrosc.* **1993**, *158*, 82.

[26] Unpublished results.

[27] Martinez III, S. J.; Alfano, J. C.; Levy, D. H. *J. Mol. Spectrosc.* **1989**, *137*, 420.

[28] In the case of L-Phe, the calculated stability of conformers was highly dependent on the calculation level. In addition, there was discrepancy between the band intensity in the electronic spectra and the relative stability calculated. As shown in Ref. 6, conformer A of L-Phe was calculated to be the ninth and fifth most stable structure at the B3LYP/6-31+G* and MP2/6-311G** levels, respectively. However, in the electronic spectra, the band of conformer A appears quite strongly; the intensity is much stronger than that estimated from Boltzmann distribution at 418 K (Ref. 6). This enhanced band intensity for conformer A of L-Phe may be due to some factors other than population of conformers, such as enhanced probability of electronic transitions for conformer A. For L-Tyr, on the contrary, the LIF spectra show strong bands of conformers B-*n* and X-*n*, which are predicted to be the most stable in DFT calculations. Therefore, it is reasonable to assign vibronic bands of L-Tyr on the basis of the total energy of stable conformers calculated at the B3LYP/6-31+G* level.

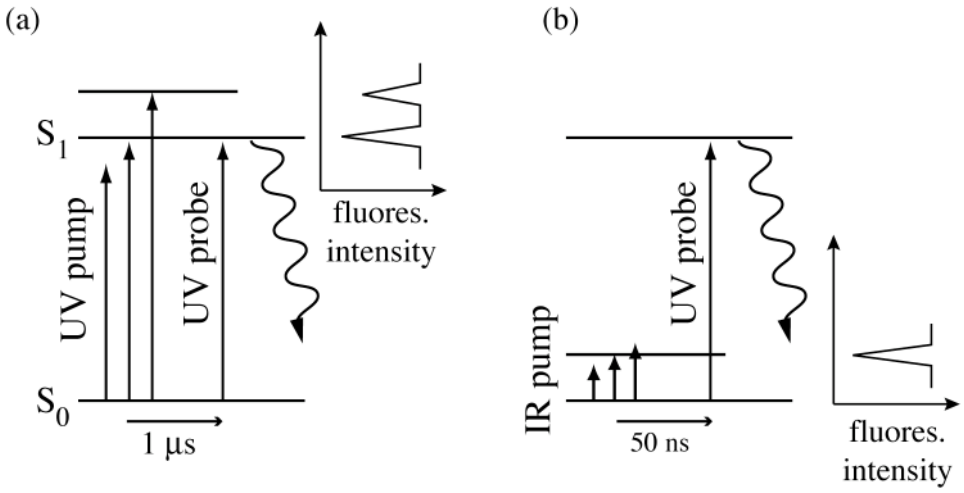

Figure 1. Inokuchi et al.

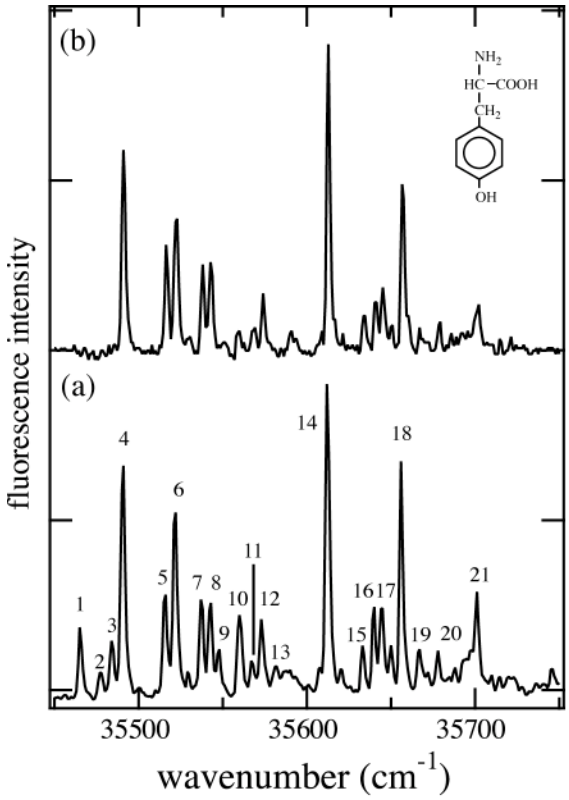

Figure 2. Inokuchi et al.

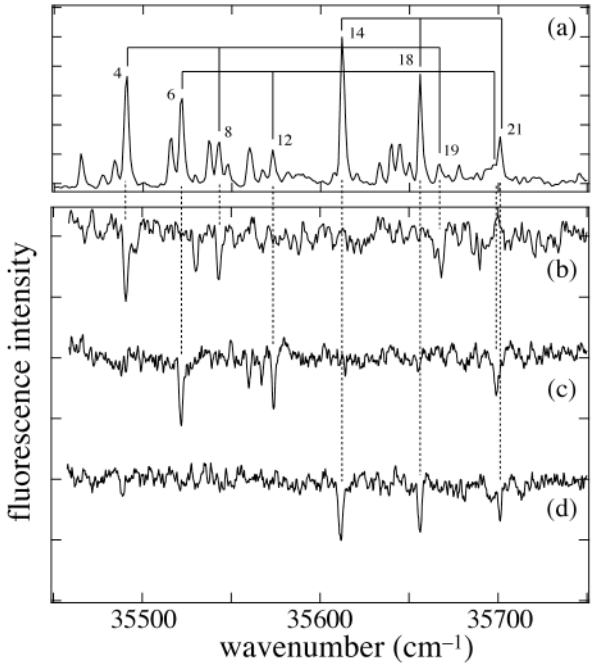

Figure 3. Inokuchi et al.

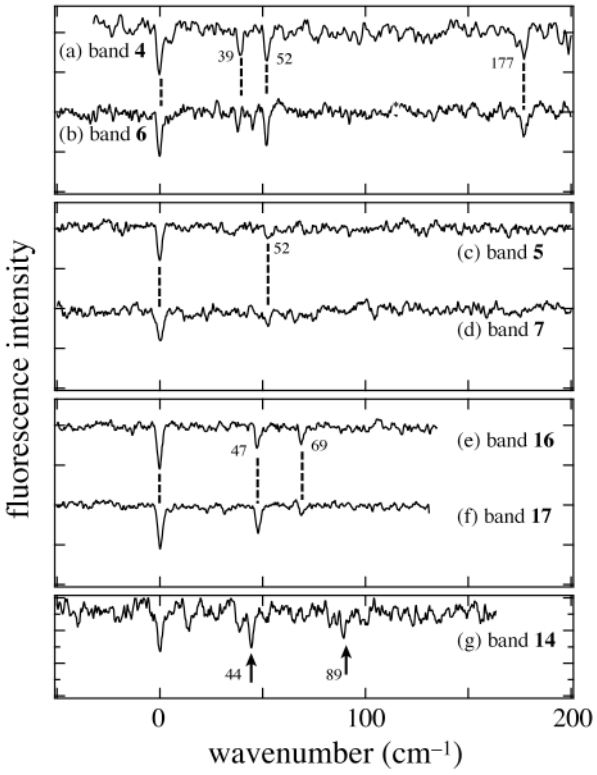

Figure 4. Inokuchi et al.

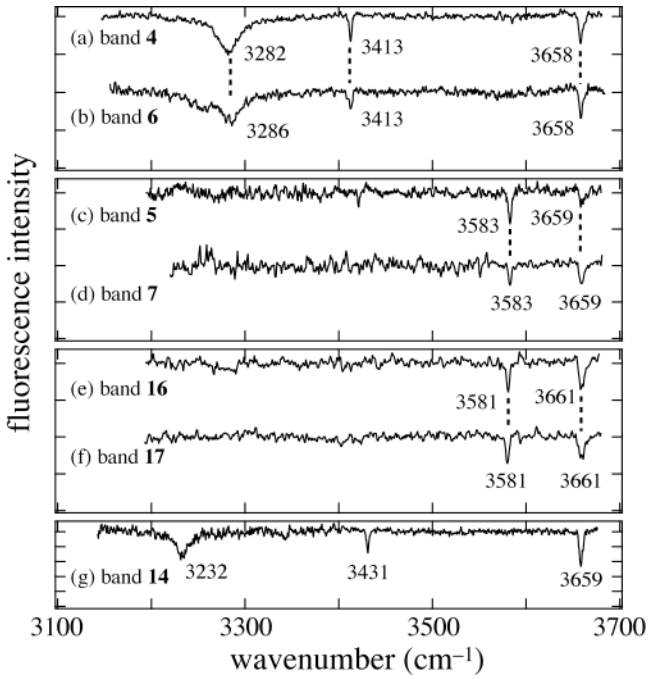

Figure 5. Inokuchi et al.

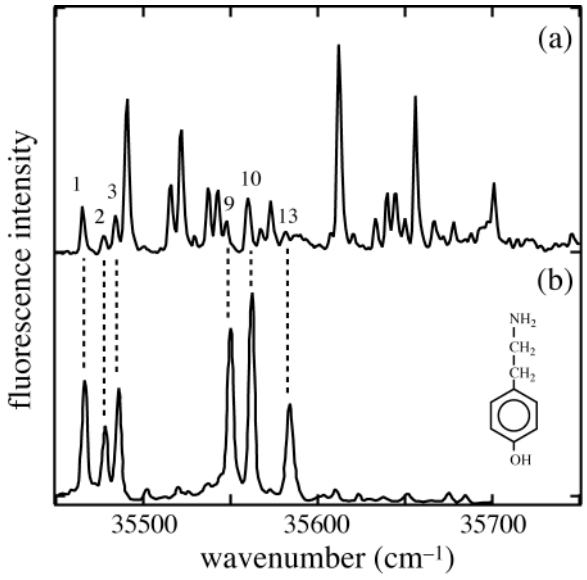

Figure 6. Inokuchi et al.

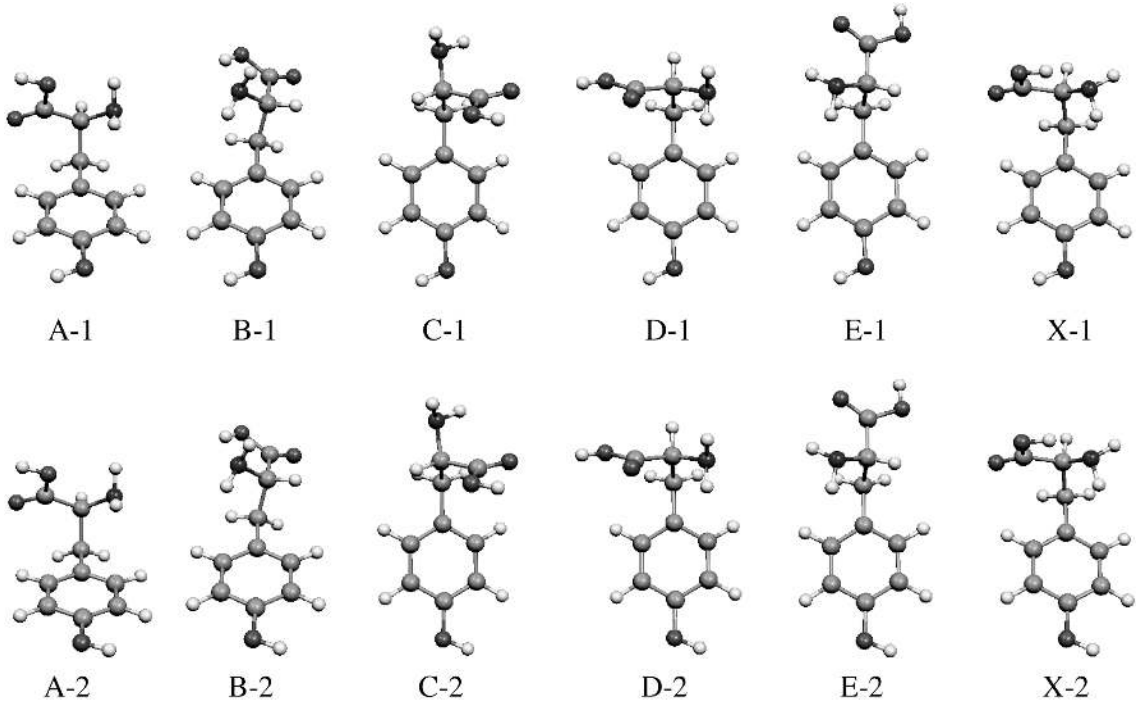

Figure 7. Inokuchi et al.

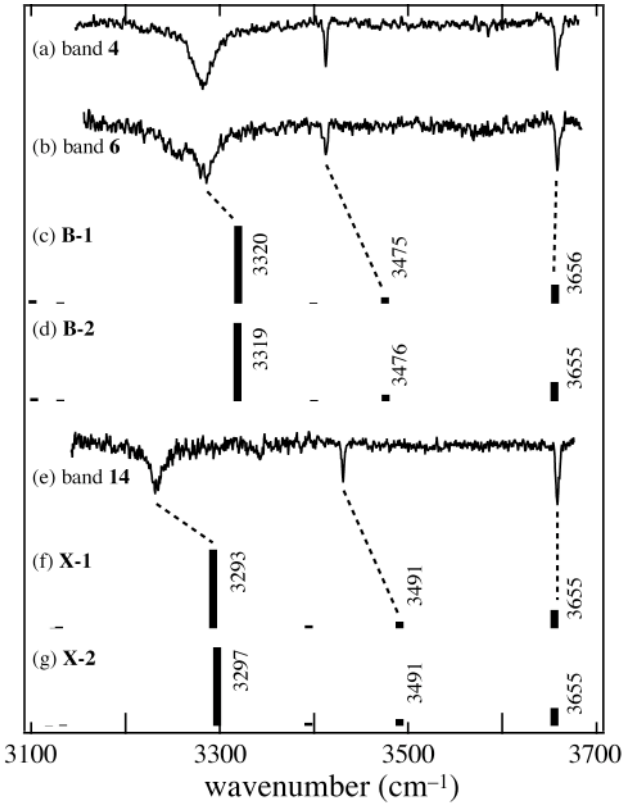

Figure 8. Inokuchi et al.

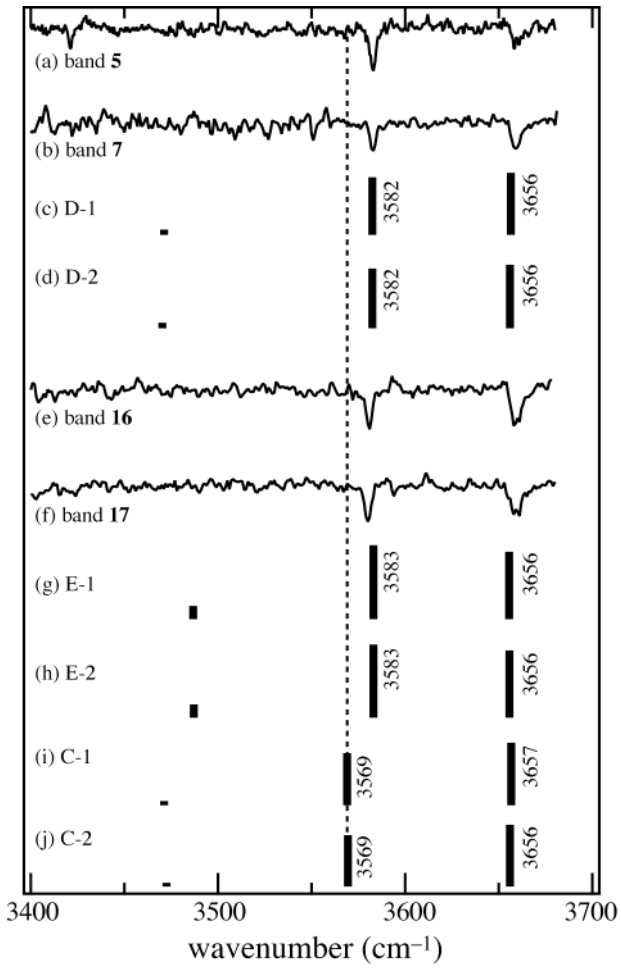

Figure 9. Inokuchi et al.

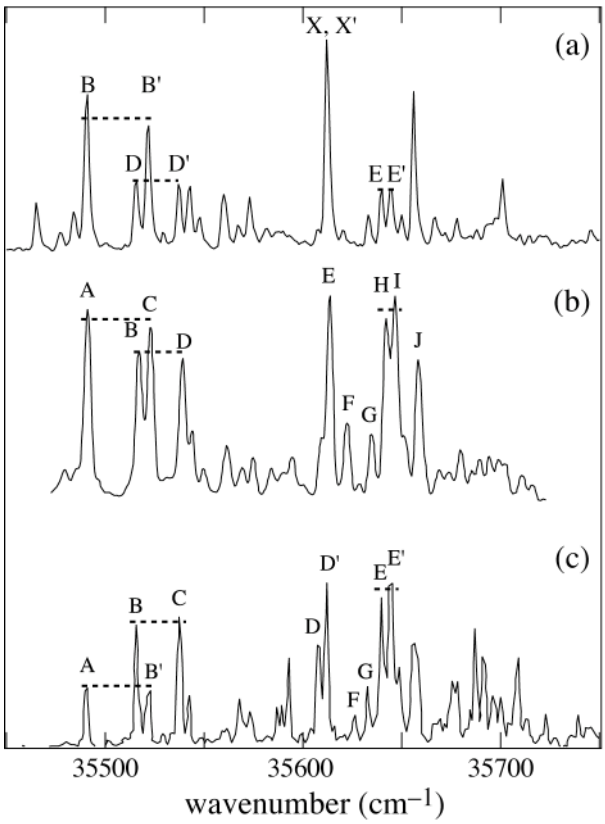

Figure 10. Inokuchi et al.